Metabolomic Profiles in Tissues of Nonhuman Primates Exposed to Either Total- or Partial-Body Radiation

Authors: Carpenter, Alana D., Li, Yaoxiang, Fatanmi, Oluseyi O., Wise, Stephen Y., Petrus, Sarah A., et al.

Source: Radiation Research, 201(5) : 371-383

Published By: Radiation Research Society

URL: https://doi.org/10.1667/RADE-23-00091.1

RADIATION RESEARCH **201**, 371–383 (2024)
0033-7587/24 $15.00

DOI: 10.1667/RADE-23-00091.1

Metabolomic Profiles in Tissues of Nonhuman Primates Exposed to Either Total- or Partial-Body Radiation

Alana D. Carpenter,[a,b,1] Yaoxiang Li,[c,1] Oluseyi O. Fatanmi,[a,b] Stephen Y. Wise,[a,b] Sarah A. Petrus,[a,b] Brianna L. Janocha,[a,b] Amrita K. Cheema,[c,d] Vijay K. Singh[a,b,2]

[a] Division of Radioprotectants, Department of Pharmacology and Molecular Therapeutics, F. Edward Hébert School of Medicine, Uniformed Services University of the Health Sciences, Bethesda, Maryland; [b] Armed Forces Radiobiology Research Institute, Uniformed Services University of the Health Sciences, Bethesda, Maryland; [c] Department of Oncology, Lombardi Comprehensive Cancer Center, Georgetown University Medical Center, Washington, DC; [d] Department of Biochemistry, Molecular and Cellular Biology, Georgetown University Medical Center, Washington DC

Metabolomic Profiles in Tissues of Nonhuman Primates Exposed to Either Total- or Partial-Body Radiation. Radiat Res. 201, 371–383 (2024).

A complex cascade of systemic and tissue-specific responses induced by exposure to ionizing radiation can lead to functional impairment over time in the surviving population. Current methods for management of survivors of unintentional radiation exposure episodes rely on monitoring individuals over time for the development of adverse clinical symptoms due to the lack of predictive biomarkers for tissue injury. In this study, we report on changes in metabolomic and lipidomic profiles in multiple tissues of nonhuman primates (NHPs) that received either 4.0 Gy or 5.8 Gy total-body irradiation (TBI) of ^{60}Co gamma rays, and 4.0 or 5.8 Gy partial-body irradiation (PBI) from LINAC-derived photons and were treated with a promising radiation countermeasure, gamma-tocotrienol (GT3). These include small molecule alterations that correlate with radiation effects in the jejunum, lung, kidney, and spleen of animals that either survived or succumbed to radiation toxicities over a 30-day period. Radiation-induced metabolic changes in tissues were observed in animals exposed to both doses and types of radiation, but were partially alleviated in GT3-treated and irradiated animals, with lung and spleen being most responsive. The majority of the pathways protected by GT3 treatment in these tissues were related to glucose metabolism, inflammation, and aldarate metabolism, suggesting GT3 may exert radioprotective effects in part by sparing these pathways from radiation-induced dysregulation. Taken together, the results of our study demonstrate that the prophylactic administration of GT3 results in metabolic and lipidomic shifts that likely provide an overall advantage against radiation injury. This investigation is among the first to highlight the use of a molecular phenotyping approach in a highly translatable NHP model of partial- and total-body irradiation to determine the underlying physiological mechanisms involved in the radioprotective efficacy of GT3. © 2024 by Radiation Research Society

INTRODUCTION

Acute radiation syndrome (ARS) in humans is an illness involving multiple organ systems caused by total- or partial-body exposure to ionizing radiation of greater than 1 Gy at a high dose rate (*1*, *2*). Individuals developing hematopoietic acute radiation syndrome (H-ARS) or gastrointestinal acute radiation syndrome (GI-ARS) may benefit from treatment with radiation medical countermeasures (MCMs), and have generally been the focus of research efforts for developing MCMs and identifying biomarkers (*3*, *4*). The development of radiation MCMs is a top priority for the U.S. Government due to the increasing risk of the detonation of improvised nuclear devices by domestic or foreign adversaries or from radiological or nuclear accidents. All four radiation MCMs currently approved by the U.S. Food and Drug Administration (FDA) are radiomitigators, which are for use after radiation exposure and prior to the onset of symptoms (*5*, *6*). One potential radiation MCM under advanced development as a pre-exposure prophylactic for H-ARS is gamma-tocotrienol (GT3) (*7*). GT3 is an antioxidant as well as an inhibitor of 3-hydroxy-3-methylglutaryl-coenzyme A reductase that has demonstrated radioprotective efficacy in both murine and nonhuman primate (NHP) models of total-body irradiation (TBI) and partial-body irradiation (PBI) when administered 24 h prior to radiation exposure (*8–15*). GT3 has been shown to modulate several biomarkers using various "omics" platforms (*16–21*). This MCM is being developed for H-ARS following the FDA Animal Rule since the efficacy of such agents cannot be investigated in a clinic under phase II and phase III trials (*22*). The NHP model is considered the gold standard of animal models for developing radiation MCMs and identifying and validating biomarkers for radiation injury and MCM efficacy (*23*, *24*).

Clinical interventions to treat ARS include the use of MCMs and other medical management options depending on the absorbed radiation dose. Therefore, it is critical to assess the extent of radiation exposure in order to provide appropriate and timely medical interventions (*25*). However, current dosimetry methods used to assess the absorbed radiation dose,

[1] These authors contributed equally to the study.
[2] Corresponding author: Vijay K. Singh, Ph.D., Division of Radioprotectants, Department of Pharmacology and Molecular Therapeutics, F. Edward Hébert School of Medicine, Uniformed Services University of the Health Sciences, Bethesda, MD; email: vijay.singh@usuhs.edu.

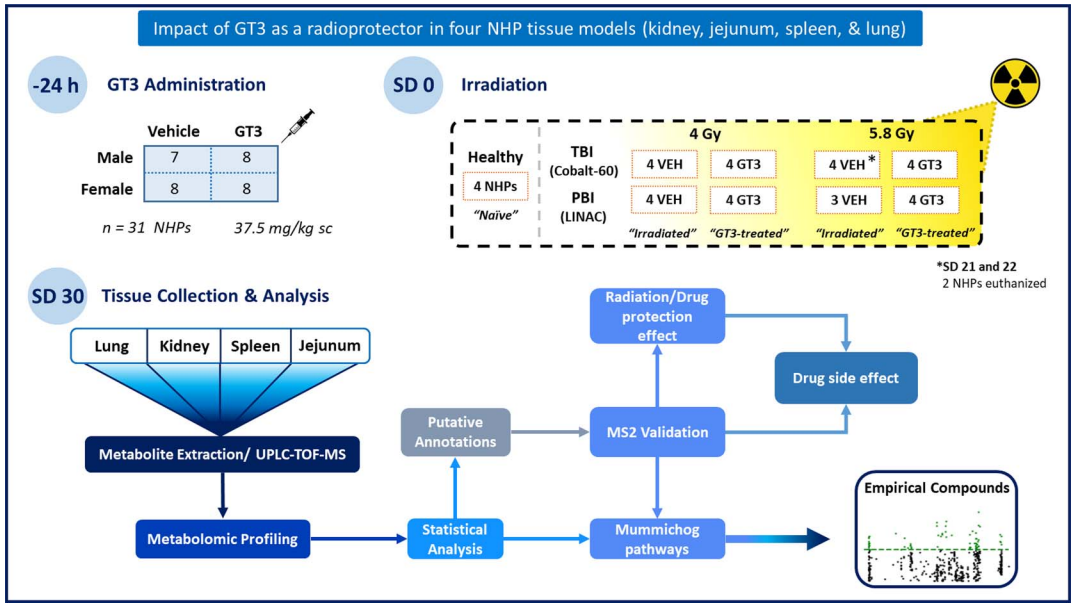

FIG. 1. Overall experimental design for the longitudinal protective effect of GT3 for different radiation types and doses.

including cytogenetic analysis of peripheral blood lymphocytes, are time-consuming, labor-intensive, and require well-trained personnel. In a large-scale radiological/nuclear event scenario, the infrastructure and personnel required to perform these assays would be scarce (*26*). Therefore, new tools that are fast and easy to perform are required to enable screening of a large number of victims so medical interventions can be provided soon after possible exposure. Some promising methods include assays involving genomic, transcriptomic, proteomic, and metabolomic biomarkers, which have the potential for high-throughput mass screening (*3*, *27–29*).

In this study, we profiled metabolomic changes in various tissues that vary in radiation sensitivity. Tissues with differing radiosensitivity were selected to assess the varying degrees of radiation injury in NHPs (rhesus macaques, *Macaca mulatta*) exposed to ARS-inducing doses of radiation, in addition to the radioprotective attributes of GT3 on an organ-specific level. Among the tissues analyzed, the jejunum is particularly radiosensitive, while the lung, kidney, and spleen are comparatively resistant to radiation injury. We expected to see minimal metabolic perturbations in the lung, spleen, and kidney, and a greater degree of dysregulation in jejunum. However, the lung and spleen showed the greatest metabolic dysregulation that was ameliorated in GT3-treated and irradiated animals.

MATERIALS AND METHODS

Experimental Design

The objective of this study was to assess tissue-specific metabolic changes in a TBI or PBI NHP model and the alleviation of radiation injury by GT3 as apparent by the correction of aberrant metabolic pathways. Four tissue types were chosen based on their varying degree of radiosensitivity. Two different doses and types of radiation were used in this study: 4.0 or 5.8 Gy of Cobalt-60 gamma rays for total-body exposure, and 4 or 5.8 Gy of LINAC-derived photons for partial-body exposure; partial-body exposure provided 5% bone marrow sparing. Both 4 (sublethal) and 5.8 Gy ($\sim LD_{30/60}$) are radiation doses known to induce H-ARS. A group of sixteen animals was randomly selected for total-body exposure to either 4.0 or 5.8 Gy; eight received GT3 [37.5 mg/kg, subcutaneously (s.c.)] and eight received an olive oil formulation vehicle (*14*). Similarly, for PBI, 15 animals were randomly divided so that eight animals received GT3 (37.5 mg/kg, s.c.), and the remaining seven animals received a vehicle. These animals were further divided so that eight animals were irradiated with 4.0 Gy PBI, and seven were exposed to 5.8 Gy partial-body irradiation. Tissue samples (jejunum, lung, kidney, and spleen) were collected at the end of the course of this 30 day study and were analyzed for comparative metabolomic profiles (*14*). The experimental design of this study is described in Fig. 1. The vehicle-treated group is referred to as the "irradiated group," and the GT3-treated groups exposed to either 4 or 5.8 Gy total-body or partial-body irradiation are referred to as "GT3," "GT3-treated," or "GT3-treated and irradiated." Healthy animals, which were used as a control for vehicle-treated, irradiated animals, are referred to as "naïve," as these animals were not exposed to radiation and did not receive any GT3 treatment.

Animals

A total of 31 naïve rhesus macaques (*Macaca mulatta*, Chinese sub-strain, 15 males and 16 females) were used for this study. The animals were between 2.5–7 years of age, weighing 4 – 8 Kg. Four animals were procured from the National Institutes of Health Animal Center (NIHAC, Poolesville, MD), and the remaining 27 were supplied by an NHP vendor (PrimGen, Hines, IL). All animals were maintained in a facility accredited by the Association for Assessment and Accreditation of Laboratory Animal Care (AAALAC)-International. Animals were quarantined for six weeks prior to the initiation of the experiment. Animal housing, health monitoring, care, and enrichment during the experimental period have been described in detail earlier (*11*, *30*). All procedures involving animals were approved by the Institutional Animal Care and Use Committee (BIOQUAL Inc., protocol #18-060) and the Department of Defense Animal Care and Use Review Office (ACURO). This study was carried out in strict accordance with the recommendations made in the Guide for the Care and Use of Laboratory Animals (*31*).

GT3 or Vehicle Preparation and Administration

GT3 and its vehicle were procured from Callion Pharma (Jonesborough, TN). The GT3 was supplied as an injectable solution at a

concentration of 50 mg/ml and an olive oil formulation was used as the vehicle. Just prior to administration, the GT3 and vehicle solution were thoroughly mixed using a laboratory vortexer. GT3 or vehicle was administered at a dose of 37.5 mg/kg s.c. 24 h prior to irradiation (*13*). Injections were performed with a sterile 21–25-gauge needle (length = 0.75–1 inch). The site for injection (midline, dorsal scapular region) was prepared as a surgical site before the injection. The exact volume administered depended on the individual weight of the NHP.

Radiation Exposure

For TBI and PBI, the high level ^{60}Co γ-radiator source and linear accelerator (LINAC) were used, respectively. The 4 Gy dose is sublethal, while the 5.8 Gy dose is low lethal ($LD_{30/60}$). Both doses of radiation induce H-ARS in an NHP model.

Total-Body Irradiation

Food was withheld from each animal approximately 12–18 h. Approximately 30–45 min prior to irradiation, NHPs were administered 10–15 mg/kg of ketamine hydrochloride intramuscularly (i.m.) for sedation. Animals were then placed in custom-made Plexiglas irradiation boxes, secured in a seated position, and irradiated with the appropriate dose (*32*). Other details of TBI and dosimetry are described earlier (*33*).

Partial-Body Irradiation

NHPs were prepared for irradiation as described above for TBI. For PBI, NHPs were irradiated one at a time using a 4 MV photon beam from an Elekta Infinity clinical LINAC. Anterior/posterior (AP) measurements of the NHPs at the location of the absorbed dose target ("core of the abdomen") were measured with a digital caliper. All other procedures of LINAC irradiation and dosimetry are discussed in a recent publication (*32*).

Euthanasia

All animals in the 4.0 Gy PBI, 4.0 Gy TBI, and 5.8 Gy PBI groups were euthanized 30 days postirradiation. In the 5.8 Gy TBI group, two female animals were euthanized early at 21 and 22 days postirradiation due to declining health. Euthanasia was carried out using the American Veterinary Medical Association (AVMA) guidelines when animals met criteria for euthanasia (*34*).

Tissue Sample Collection

The lung, spleen, jejunum, and kidney were collected from euthanized animals 30 days postirradiation (days 21 and 22 postirradiation for two animals in the 5.8 Gy TBI group). As soon as the tissue samples were harvested, all samples were transferred into individual sterile storage tubes and placed on dry ice or liquid nitrogen. Tissue samples were stored at –70°C until shipped on dry ice to Georgetown University Medical Center, Washington, DC.

Sample Preparation and LC-MS Analyses

For metabolomic analysis, tissue samples were prepared as previously described (*20*).

Statistical Analyses

Centroided and integrated mass spectrometry data from the UPLC-TOFMS were preprocessed using XCMS software (Scripps Research Institute, La Jolla, CA) to generate a data matrix containing ion intensities, mass to charge (m/z) and retention time values. The data were normalized to the intensities of internal standards and protein quantification. Multivariate statistics were performed using R scripts developed in-house (*35*) with pareto scaling and log-transformation used for data normalization. An ANOVA and Student's t-test comparisons were used to identify significantly dysregulated metabolites (based on m/z values) between comparative groups, and were further corrected using the Benjamini-Hochberg (FDR) multiple testing correction method, and were then subjected to a database search for identification and biological relevance using METLIN (*36*), CEU Mass Mediator (*37*), and HMDB (*38*). The identity of these significantly dysregulated metabolites were identified using Mummichog empirical compounds (Supplementary Table S1;[3] https://doi.org/10.1667/RADE-23-00091.1.S1) (*39*). Figures were generated using custom R scripts.

Results

GT3 is being developed using both murine and NHP as a potential prophylactic treatment for H-ARS following the U.S. FDA Animal Rule, and it has been shown to increase survival and hematopoietic recovery in lethally irradiated animals (*8*). To understand the mechanisms by which GT3 exerts its radioprotective effects at the metabolic level and to identify its biomarkers, tissues from vital organs were sampled for metabolomic analysis following GT3 treatment and irradiation (Fig. 1). The number and classes of metabolites analyzed varied depending on tissue type, and a comprehensive list of all metabolites analyzed is detailed in Supplementary Table S1 (https://doi.org/10.1667/RADE-23-00091.1.S1).

Radiation-Induced Robust Changes Across all Tissue Types Analyzed

To determine the effects of either 4.0 or 5.8 Gy of gamma radiation in a PBI or TBI model on jejunum, kidney, lung, and spleen, samples collected at the time of euthanasia (SD30 unless otherwise noted) from the irradiated group were compared to naïve samples. Untargeted metabolomics data pathway analysis was performed using Mummichog 2.06 software (http://mummichog.org/). Radiation-induced dysregulation in metabolomic profiles was visualized as volcano plots for all four tissues at 30 days postirradiation (Fig. 2). A comprehensive list of all metabolites and pathways analyzed for each comparison can be viewed in Supplementary Tables S2–S9 (https://doi.org/10.1667/RADE-23-00091.1S1).

Jejunum

The jejunum is a known radiosensitive organ, and therefore more robust changes in metabolic pathways were expected, and in a radiation dose-dependent manner. Overall, animals exposed to 5.8 Gy experienced a greater dysregulation of metabolic pathways when compared to animals exposed to 4 Gy; however, there was little overlap in significant pathways between the two radiation groups suggesting that radiation dose can impact metabolic response. There were a few commonalities in significantly dysregulated metabolites between radiation dose groups. Hexadecanoic acid and octadecatrienoic acid were significantly dysregulated in all groups, apart from animals exposed to 5.8 Gy PBI. Similarly, L-gulonate, deoxyguanosine, and hypoxanthine were dysregulated in all groups except animals receiving 5.8 Gy TBI. Phytosphingosine, 4,8 dimethylnonanoyl carnitine, and octadecatrienoic acid were dysregulated by the lower dose of radiation (4 Gy TBI and PBI), while 5′-phosphoribosylglycinamide was dysregulated by the higher dose (5.8 Gy TBI or PBI). Several pathways common to this tissue were dysregulated by radiation exposure including bile acid biosynthesis and pentose and glucoronate interconversion pathways. These two pathways were significantly dysregulated in all groups except for animals receiving a 5.8 Gy TBI dose. The pentose phosphate pathway was dysregulated only in animals undergoing PBI, while the linoleate metabolism pathway was dysregulated only in the TBI groups. Purine metabolism, N-glycan biosynthesis, and vitamin B9 (folate) metabolism pathways were dysregulated only in animals exposed to 5.8 Gy. Pathways including the vitamin A (retinol) metabolism, vitamin K metabolism, and fatty acid oxidation pathways, which primarily occur in hepatic tissue, were significantly dysregulated in jejunal tissue; however, these were primarily isolated events, and these pathways were not commonly

[3] Editor's note. The online version of this article (DOI: https://doi.org/10.1667/RADE-23-00091.1) contains supplementary information that is available to all authorized users.

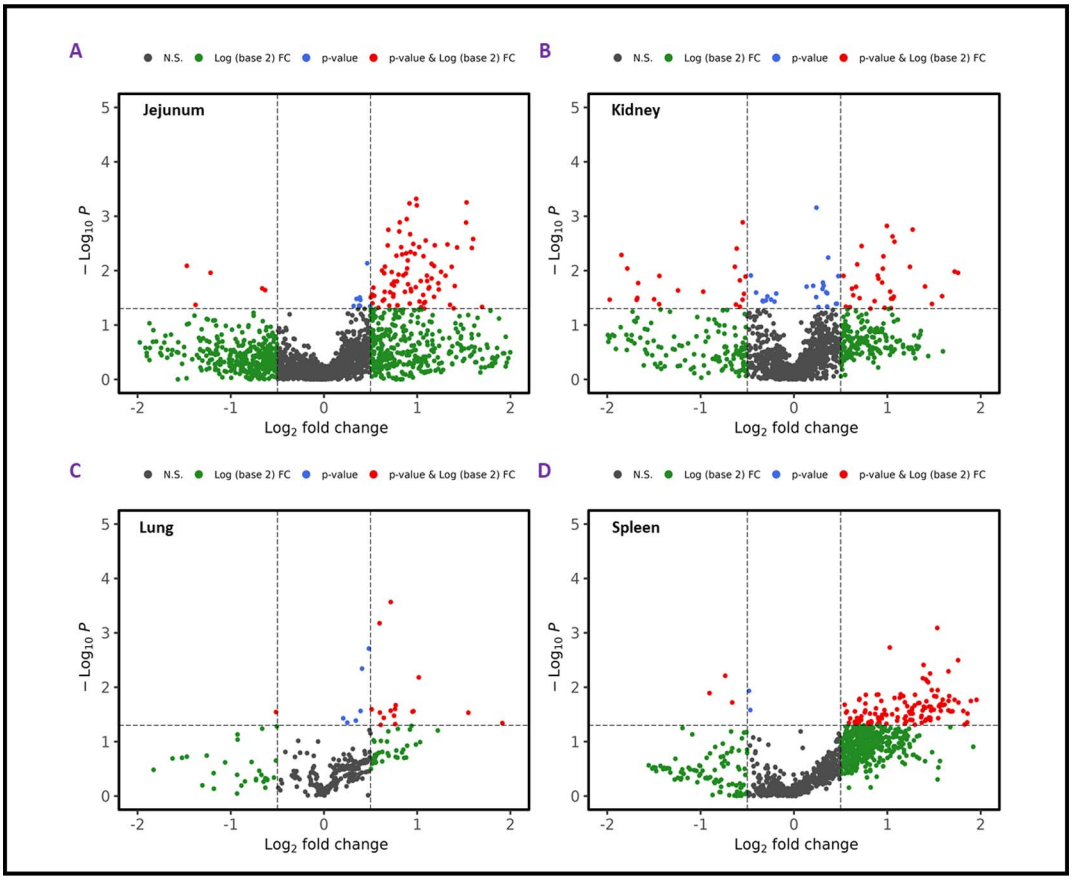

FIG. 2. Volcano plot showing comparison of metabolic profiles of NHP tissue exposed to 4.0 Gy PBI at SD30: jejunum (panel A), kidney (panel B), lung (panel C), and spleen (panel D).

dysregulated between radiation exposure types or doses. Interestingly, contrary to what we expected, a larger perturbation in metabolites was observed in animals exposed to 4 Gy when compared to their 5.8 Gy counterparts. A comprehensive list of all metabolites and pathways analyzed in jejunum can be viewed in Supplementary Tables S2 and S6 (https://doi.org/10.1667/RADE-23-00091.1.S1).

Kidney

Similar to our observations in the jejunum, a large number of dysregulated metabolites were observed in the 5.8 Gy TBI group. However, only one metabolite, prostaglandin E2, was significantly dysregulated across all irradiated groups. Threonate was significantly disrupted in all groups except the 4 Gy PBI group. Within both 4 Gy exposure groups, creatine was significantly perturbed, while 5-phenyl-1,3-oxazinane-2,4-dione was only dysregulated by TBI, and deoxyuridine was dysregulated by PBI (both 4 and 5.8 Gy). In the animals exposed to 5.8 Gy, L-erythrulose was significantly perturbed in both exposure groups. Other irregularities found in the 5.8 Gy TBI group include 5(S)-HETE, 9(S)-HETE, and substituted octadecatrienoic acid. As expected, pathways were dysregulated in a radiation dose dependent manner, with the 5.8 Gy TBI group having the largest amount of irregularities. Generally, ascorbate (vitamin C) and aldarate metabolism, arginine and proline metabolism, starch and sucrose metabolism, and prostaglandin formation from arachidonate were significantly dysregulated among irradiated animals; however, few similarities between irradiated groups were observed. Except for 4 Gy PBI groups, all irradiated groups displayed significant deviations in the starch and sucrose metabolism pathway, and prostaglandin formation from the arachidonate pathway was commonly dysregulated in both 4 Gy exposure groups. A comprehensive list of dysregulated metabolites is detailed in Supplementary Tables S3 and S7 (https://doi.org/10.1667/RADE-23-00091.1.S1).

Lung

Lung metabolomics revealed similar levels of metabolite perturbations between the four irradiated groups; however, the majority of deviations were unique to each group. Four metabolites were significantly dysregulated in all of the irradiated groups. Clupanodonyl carnitine and prostaglandin-PGB2-glyceryl ester were significantly perturbed in all groups except for 4 Gy PBI, and protoporphyrinogen IX and bilirubin were significant in all groups except for 5.8 Gy PBI and TBI, respectively. Hexadecanoic acid, selenohomocysteine, prostaglandin E2, and icosatetraenoic acid were significantly dysregulated by the lower doses of radiation (4 Gy PBI and TBI), while timnodonyl carnitine and homovanillin were exclusively affected by the higher doses of radiation (5.8 Gy PBI and TBI). Linoelaidyl carnitine was uniquely significant to TBI, but no metabolites were unique to PBI in the lung. Interestingly, we found that the 4 Gy PBI group had the greatest amount of significantly dysregulated pathways. Only one pathway was significantly perturbed across all irradiated groups: androgen and estrogen biosynthesis and metabolism. With the exception of the 4 Gy PBI group, C21-steroid hormone biosynthesis and metabolism was significantly different in all irradiated groups in comparison to naïve animals. The greatest number of similarities was within the 4 Gy exposure groups, which shared dysregulation of numerous metabolic fatty acid pathways, including fatty acid activation and metabolism, selenoamino acid metabolism, de novo fatty acid biosynthesis, and saturated fatty acid beta-oxidation pathways, in addition to prostaglandin formation from arachidonate. Pulmonary metabolite and pathway analysis results can be viewed in

Supplementary Tables S4 and S8 (https://doi.org/10.1667/RADE-23-00091.1.S1), respectively.

Spleen

The greatest amount of metabolite dysregulation was found in the 4 Gy TBI group, while the 5.8 Gy TBI group had the least number of disturbances comparatively. A total of five metabolites were significantly dysregulated in all irradiated groups, including (S)-1-pyrroline-5-carboxylate, D-galactose, UDP-N-acetyl-D-galactosamine, sphingosine 1-phosphate, and androsterone glucuronide. N-formimino-L-glutamate, bilirubin, D-erythrose 4-phosphate, and D-ribose were exclusively significant in animals exposed to PBI, and 3-carbamoyl-2-phenylpropionic acid, sphinganine, 8alpha-hydroxytocopherone, and phytosphingosine were significantly different in response to TBI. L-Threonate was the only metabolite that was exclusive to 5.8 Gy, while there were 12 metabolites commonly dysregulated in the 4 Gy groups. Among these are prostaglandin B2, C2, and E2, Hepoxilin A3, Epoxy-8-hydroxyicosa-5,9,14-trienoic acid, and ketoleucine (4-Methyl-2-oxopentanoate). The greatest amount of perturbations in metabolic pathways was both dose and exposure dependent with the greatest changes found in the 5.8 Gy TBI group. Four pathways were significant across all irradiated groups, including glycosphingolipid metabolism, keratan sulfate degradation, N-Glycan biosynthesis, and phosphatidylinositol phosphate metabolism. Squalene and cholesterol biosynthesis, prostaglandin formation from arachidonate, androgen and estrogen biosynthesis and metabolism, and histidine metabolism were exclusively dysregulated in animals exposed to the lower doses of radiation (4 Gy PBI and TBI), while ascorbate (vitamin C) and aldarate metabolism and porphyrin metabolism were disrupted only in the higher radiation dose groups (5.8 Gy PBI and TBI). Three pathways including arginine and proline metabolism, sialic acid metabolism, and glycine, serine, alanine, and threonine metabolism were significantly different in response to PBI, while no pathways were exclusively significant different to TBI. A comprehensive list of all metabolites and pathways analyzed in splenic tissue can be viewed in Supplementary Tables S5 and S9 (https://doi.org/10.1667/RADE-23-00091.1.S1), respectively.

Animals exposed to 4 Gy experienced less metabolic disruption when compared to animals exposed to 5.8 Gy, and animals exposed to TBI experienced more deleterious effects of radiation compared to animals exposed only to PBI. There were some overlapping responses to radiation within the four tissue types; however, most of the instances were inconsistent in terms of radiation dose and exposure type. Metabolic perturbations were more pronounced in the 4 Gy groups compared to the 5.8 Gy groups in both jejunum and spleen. Lung and kidney tissue experienced minimal radiation-induced metabolic perturbations, with the 5.8 Gy groups experiencing the largest degree of dysregulation. The lung and spleen were the most sensitive to radiation, and showed the greatest degree of metabolic dysregulation overall compared to the other tissues. Of the commonly dysregulated pathways with comparable effects, the C21-steroid hormone biosynthesis and metabolism pathway was the only pathway that was dysregulated in all four tissues; specifically, there was significant dysregulation in the 4 Gy PBI groups in the kidney and spleen, the 4 Gy TBI groups in the jejunum and lung, and in both 5.8 Gy PBI and TBI groups in the lung. Prostaglandin formation from arachidonate was dysregulated in the 4 Gy PBI and TBI groups of the lung, kidney, and spleen. Glycosphingolipid metabolism was dysregulated in all irradiated groups in the spleen, 4 Gy PBI in the lung, and both 4 Gy groups in the jejunum as well as 5.8 Gy TBI.

GT3 Provided Robust Protection in Lung and Spleen Tissue

To determine the effects of 4.0 or 5.8 Gy PBI or TBI, jejunum, kidney, lung, and spleen tissue samples collected at the time of euthanasia from the GT3-treated and irradiated groups were compared to the irradiated groups. We expected to see a greater degree of dysregulation in animals exposed to 5.8 Gy compared to 4.0 Gy, with TBI causing greater metabolic perturbations compared to PBI. GT3 was expected to mitigate this dysregulation. However, this trend was not observed in some tissues, as discussed below (Fig. 3). A list of metabolites that were protected by GT3 treatment in each tissue can be viewed in Table 1.

Jejunum

GT3 treatment was found to significantly modulate some biochemical pathways in jejunal tissue; however, there was little overlap between treatment groups. The greatest variation in the metabolome was found within the jejunum of the GT3-treated and irradiated animals, which can primarily be attributed to the 4 Gy PBI exposure group; interestingly, a total of 52 metabolites were statistically significant in GT3-treated and irradiated animals compared to irradiated animals, while only 19 metabolites were significantly different in irradiated animals compared to naïve animals. Of these significant metabolites, six were protected by GT3 administration (including hypoxanthine, heptadecanoyl carnitine, and cholate). In the 4 Gy TBI comparison, 37 total metabolites were significantly dysregulated in irradiated animals, and only 4 metabolites showed a significant difference in GT3-treated and irradiated animals compared to irradiated animals. Only one metabolite, phytanate, was significantly protected by GT3 treatment. Interestingly, at the higher dose of radiation (the 5.8 Gy PBI and TBI comparisons), no metabolites were significantly protected by GT3 treatment. In the 5.8 Gy PBI group, 13 metabolites were significant in irradiated vs. naïve animals, while none were noted in GT3-treated and irradiated animals compared to irradiated animals. For the 5.8 Gy TBI comparison, nine unique metabolites were dysregulated in irradiated animals, and 7 total unique metabolites were significant in GT3-treated and irradiated animals compared to irradiated animals. These results suggest that GT3 is capable of providing modest protection to jejunum at lower doses of PBI, but radioprotection is minimal at the higher dose of radiation used in this study (5.8 Gy).

There were few similarities in significant pathways between the four GT3-treated and irradiated groups, and all of these similarities were in the 4 Gy PBI group; this group had 29 significantly different pathways in the irradiated vs. GT3 comparison, and 9 significantly different pathways in the irradiated vs. naïve comparison. Three pathways were commonly significant in both the irradiated vs. naïve and irradiated vs. GT3 comparisons in animals exposed to 4 Gy PBI: glycospingolipid metabolism, carnitine shuttle, and bile acid biosynthesis. Additionally, pyrimidine metabolism was commonly protected in GT3-treated and irradiated animals exposed to either 4 Gy total- or partial-body irradiation. There was no statistical significance found between the irradiated animals. and the GT3-treated and irradiated animals exposed to 5.8 Gy PBI. Select metabolites and pathways in jejunum can be viewed in Supplementary Figs. S1 and S2 (https://doi.org/10.1667/RADE-23-00091.1.S2, respectively).

Kidney

In animals exposed to 4 Gy PBI, 9 unique metabolites were significantly dysregulated by radiation, while 5 unique metabolites were significantly dysregulated in GT3-treated and irradiated animals. Of these metabolites, none were significantly protected by GT3 treatment. In the groups exposed to 4 Gy TBI, 7 metabolites were significantly dysregulated in irradiated animals, and 12 were significantly dysregulated in GT3-treated and irradiated animals; two of these metabolites, morphine-3-glucuronide and 5-phenyl-1,3-oxazinane-2,4-dione, were significantly protected. Three metabolites were significantly altered by the administration of GT3 in the 5.8 Gy PBI group, while 6 were significantly dysregulated in irradiated animals; no commonalities were noted in group-wise comparisons. As expected, a large number of metabolites were dysregulated by 5.8 Gy TBI, with 25 dysregulated metabolites. In contrast, only 5 metabolites were significantly dysregulated in GT3-treated and irradiated animals. In this comparison, two metabolites were significantly protected by GT3 administration: N-Acetyl-D-galactosamine 6-phosphate and 17-peroxy-docosahexaenoate. Interestingly, the majority of dysregulated metabolites were unique to each comparison group, with few protected metabolites in each comparison. No single metabolite was commonly protected between comparison groups in kidney.

Minimal significant pathway overlap between the irradiated vs. naïve and irradiated vs. GT3-treated and irradiated groups were noted. Overall, there was only one pathway that had shared significance between groups that were treated with GT3 and subsequently

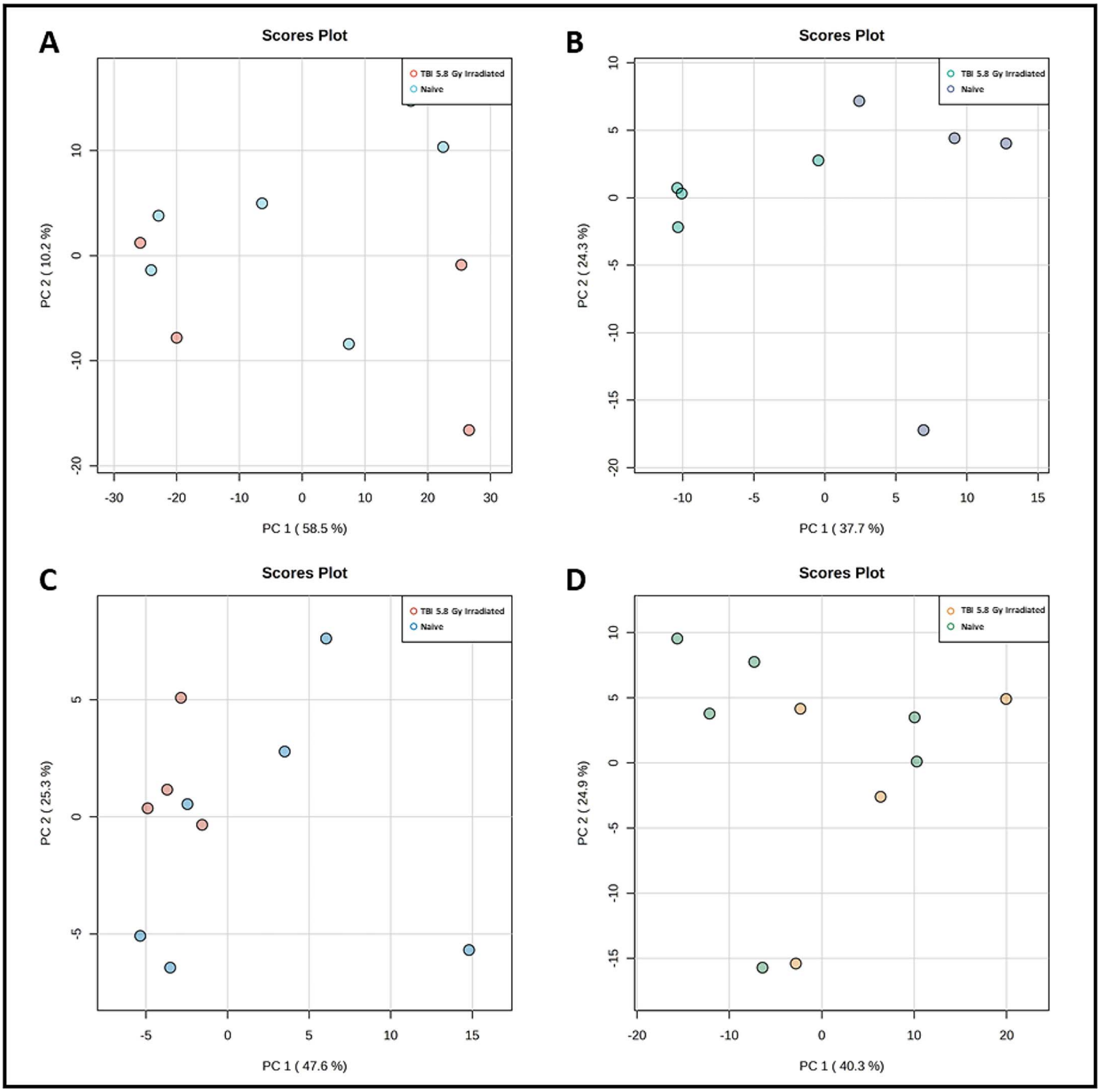

FIG. 3. Radiation (5.8 Gy TBI) induced short term (SD 30) changes in tissue metabolomic profiles in NHPs. Two-principal component analysis of two-dimensional score plots for jejunum (panel A), kidney (panel B), lung (panel C), and spleen (panel D).

irradiated, while the rest of the significance was unique to each exposure group. In both GT3-treated and irradiated groups exposed to 4 Gy, drug metabolism – cytochrome P450 was significantly altered in comparison to the corresponding irradiated groups. Both groups irradiated with 5.8 Gy had six significant dysregulated pathways, none of which were shared. Among the dysregulated pathways in the PBI group were vitamin A metabolism, vitamin B2 metabolism, glutathione metabolism, and glutamate metabolism. In the TBI group, drug metabolism – other enzymes, fructose and mannose metabolism, and sialic acid metabolism were significantly modulated by GT3 administration. These results suggest that GT3 activates unique pathways in kidney. However, the protection provided by GT3 is modest at best, and is limited to the lower radiation dose (4 Gy). These results suggest minimal protection was afforded by GT3 administration in kidney. Select metabolites and pathways in kidney can be viewed in Supplementary Figs. S3 and S4 (https://doi.org/10.1667/RADE-23-00091.1.S2).

Lung

Given that this organ is not thought to be particularly sensitive to ionizing radiation within the short-term, we expected to see minimal metabolic perturbations within lung. However, we observed a fair amount of dysregulation caused by radiation exposure, along with significant changes in metabolic profiles due to GT3 administration.

TABLE 1
Significantly Protected Metabolites by GT3 Treatment in the Various Tissues Analyzed

Metabolites	KEGG ID	m/z	RT	Fold change: 4 Gy P values: PBI irradiated vs. naïve	Fold change: 4 Gy P values: PBI irradiated vs. GT3
Jejunum					
Hypoxanthine	C00262	137.0458	0.46	↑0.011145	↓0.002584
Beta-D-mannosyldiacetylchitobiosyldiphosphodolichol	C05860	1069.4723	11.82	↑0.0048933	↓0.0095699
Heptadecanoyl carnitine	hpdcacrn	414.3596	6.57	↑0.0099747	↓0.027132
L-palmitoylcarnitine	C02990	400.3413	6.34	↑0.026311	↓0.022934
Cholate	C00695	407.2792	5.05	↑0.039523	↓0.025839
3beta-hydroxyandrost-5-en-17-one 3-sulfate (DHEA-S)	C04555	368.161	4.47	↑0.04652	↓0.030057
Phytanate	CE2414	334.2819	8.46	↓0.46347	↓0.39325
Kidney					
Morphine-3-glucuronide	C16643	462.1772	4.03	↓0.011003	↑0.28332
5-phenyl-1,3-oxazinane-2,4-dione	C16596	174.0546	1.42	↓0.057978	↑0.92942
N-Acetyl-D-galactosamine 6-phosphate	C06376	360.0692	0.45	↓0.36281	↑0.64759
17-peroxy-docosahexaenoate	CE6435	339.1995	10.29	↑0.65196	↓0.73016
Lung					
Biliverdin	C00500	583.2561	5.21	↑0.048188	↓0.006302
Timnodonate	CE2540	324.2083	8.6	↑0.0041823	↓0.012986
3-dehydrosphinganine	C02934	322.2715	5.75	↑0.014342	↓0.013626
Inosine	C00294	267.0734	0.44	↓0.95979	↓0.23538
Spleen					
Androsterone	C00523	271.2059	4.56	↑0.021531	↓0.60763
Thromboxane B2	C05963	351.2171	4.56	↑0.020861	↓0.58006
Prostaglandin B2	C05954	315.1961	4.56	↑0.020215	↓0.54752
Prostaglandin E2	C00584	375.215	4.88	↑0.00039815	↓0.43663
3beta-Hydroxyandrost-5-en-17-one	C01227	289.2167	4.56	↑0.024666	↓0.56607
Bilirubin	C00486	607.2535	8.73	↑0.021758	↓0.95755
D-galactose	C00124	195.0502	0.42	↑0.0050959	↓0.55456
1-phosphatidyl-D-myo-inositol	C01194	194.0198	0.44	↑0.015634	↓0.43776

Note. RT: retention time

Generally speaking, irradiated animals experienced a greater dysregulation of the lung metabolome compared to GT3-treated and irradiated animals. Animals exposed to TBI showed the greatest amount of metabolic disruptions when compared to their respective groups exposed to PBI. A total of 25 and 24 unique metabolites were dysregulated by 4 and 5.8 Gy TBI, respectively. Of these metabolites, 8 were commonly dysregulated by TBI; this includes androsterone, linoelaidyl carnitine, protoporphyrinogen IX, dihydrotestosterone glucuronide, Etiocholanolone glucuronide, 5,6-epoxy-alpha-tocopheryl quinone, prostaglandin-PGB2-glyceryl ester, and clupanodonyl carnitine. As for animals exposed to 4.0 and 5.8 Gy PBI, 22 and 20 metabolites, respectively, were significantly dysregulated. As previously mentioned, fewer metabolites were significantly dysregulated in GT3-treated and irradiated animals, with 5 and 16 unique significant metabolites in the 4.0 and 5.8 Gy PBI groups. In the 4 Gy PBI comparison, three metabolites including biliverdin, timnodonate, and 3-dehydrosphinganine were significantly protected by GT3 treatment, and in the 5.8 Gy PBI comparison, only one metabolite was significantly protected by GT3 treatment (inosine). Top metabolites were selected which illustrate the effects of radiation and GT3 treatment (Fig. 4).

In the 4 Gy PBI groups, the putative anti-inflammatory metabolites formed from the EPA pathway were commonly significant in the irradiated vs. naïve and irradiated vs. GT3-treated and irradiated groups. This pathway was also significant in GT3-treated and irradiated animals in the 4 Gy TBI and the 5.8 Gy PBI comparisons, but not in their respective irradiated vs. naïve groups. In the 5.8 Gy PBI comparison, the purine metabolism, tyrosine metabolism, androgen and estrogen biosynthesis and metabolism, and urea cycle/amino group metabolism pathways were commonly significant in the irradiated vs. naïve and irradiated vs. GT3-treated and irradiated groups, suggesting GT3 played a protective role in these pathways. Five pathways were common between the 4 Gy TBI and 5.8 PBI GT3 groups, including purine metabolism, urea cycle/amino group metabolism, glutathione metabolism, aspartate and asparagine metabolism, and putative anti-inflammatory metabolites formation from EPA. Both groups exposed to total-body irradiation shared two significant pathways: vitamin B5 metabolism and CoA catabolism. Selected

TABLE 1
Extended.

Fold change					
4 Gy P values		5.8 Gy P values			
TBI irradiated vs. naïve	TBI irradiated vs. GT3	PBI irradiated vs. naïve	PBI irradiated vs. GT3	TBI irradiated vs. naïve	TBI irradiated vs. GT3
Jejunum					
↑0.040569	↑0.25074	↑0.045682	↓0.39895	↑0.70662	↑0.95505
↑0.31182	↓0.85315	↑0.24797	↓0.45436	↑0.03806	↓0.2251
↑0.12344	↑0.40104	↑0.069869	↓0.33251	↑0.39635	↓0.80398
↑0.53006	↑0.18676	↑0.029837	↓0.3385	↑0.19356	↓0.62757
↑0.6683	↓0.55325	↑0.13614	↓0.72307	↑0.34978	↓0.83926
↓0.92977	↑0.3188	↑0.20541	↓0.31137	↑0.28698	↓0.79596
↓0.023781	↑0.043739	↓0.46147	↓0.4292	↓0.53775	↓0.69251
Kidney					
↓0.009624	↑0.047472	↓0.21804	↑0.71583	↓0.08385	↓0.7124
↓0.004113	↑0.00925	↓0.06743	↑0.23064	↓0.01903	↑0.79265
↓0.57863	↑0.56617	↑0.32771	↓0.060933	↑0.00658	↓0.018311
↑0.63386	↑0.68146	↑0.07304	↑0.95987	↑0.00181	↓0.016135
Lung					
↑0.15112	↓0.34289	↑0.19395	↑0.46091	↑0.42251	↑0.2931
↑0.24312	↓0.29546	↑0.16045	↑0.53697	↑0.25377	↑0.85381
↑0.12448	↓0.4201	↑0.89142	↑0.27039	↑0.37071	↑0.064461
↓0.44819	↓0.91167	↑0.012124	↓0.02261	↑0.17385	↑0.39547
Spleen					
↑0.026824	↓0.043787	↑0.2081	↓0.47056	↑0.60709	↑0.14559
↑0.029157	↓0.048981	↑0.19851	↓0.42798	↑0.5321	↑0.17807
↑0.029956	↓0.048463	↑0.20835	↓0.47891	↑0.5439	↑0.17051
↑0.001115	↓0.10719	↑0.01565	↓0.75116	↑0.097108	↑0.19503
↑0.030309	↓0.042234	↑0.18449	↓0.40289	↓0.62551	↑0.44279
↑0.057174	↑0.26702	↑0.0085151	↓0.043144	↑0.14452	↓0.8086
↑0.010859	↓0.58252	↑0.0026574	↓0.025189	↑0.0079918	↑0.48187
↑0.030745	↓0.43237	↑0.031497	↓0.036158	↑0.13022	↑0.31461

significant pathways altered by radiation exposure and GT3 treatment can be viewed in Fig. 5.

Spleen

Metabolic profiles in spleen followed a similar trend, and dysregulation was higher in irradiated animals compared to GT3-treated and irradiated animals. A total of 40 metabolites were significantly dysregulated in irradiated animals exposed to 4 Gy PBI, compared to only one unique significant metabolite in the GT3-treated and irradiated animals. For animals exposed to 4 Gy TBI, 47 metabolites were significantly dysregulated when comparing naïve and irradiated animals, while 13 metabolites showed a significant difference between the irradiated animals and the GT3-treated and irradiated animals. Interestingly, 5 total metabolites were significantly protected by GT3 treatment: androsterone, thromboxane B2, prostaglandin B2, prostaglandin E2, and 3beta-Hydroxyandrost-5-en-17-one. Fewer metabolites were significantly dysregulated in PBI groups when compared to their TBI equivalents. Irradiated and GT3-treated and irradiated animals in the 5.8 Gy PBI groups had a total of 21 and 7 significant metabolites, respectively, 4 of which were protected by GT3 treatment: thromboxane B2, D-galactose, 1-phosphatidyl-D-myo-inositol, and bilirubin. Twenty metabolites were significantly dysregulated in animals that received 5.8 Gy TBI, and 2 were significant in GT3-treated and irradiated animals; however, no metabolites were protected in this group. Thromboxane B2 was the only metabolite that was significantly protected by GT3 treatment in more than one group (4 Gy TBI and 5.8 Gy PBI).

A greater number of pathways were significantly different in the irradiated vs. naïve comparisons than in the irradiated vs. GT3 comparisons. Twenty-two metabolic pathways were significant in the animals exposed to 4 Gy PBI in comparison to only one uniquely significant pathway in GT3-treated and irradiated animals. Animals exposed to 4 Gy TBI had significant changes in 28 metabolic pathways, and 7 significant pathways in the GT3-treated and irradiated animals; two, including prostaglandin formation from arachidonate and androgen and estrogen biosynthesis and metabolism, were commonly significant. The greatest degree of protection was observed in the 5.8 Gy PBI groups. A total of 24 pathways were significantly dysregulated in the 5.8 Gy PBI irradiated animals, and 15 were significantly dysregulated in GT3-treated and irradiated animals; 8 of these pathways were also commonly significant, including sialic acid metabolism, pentose phosphate pathway, chondroitin sulfate degradation, heparan sulfate degradation, pentose and glucoronate interconversions,

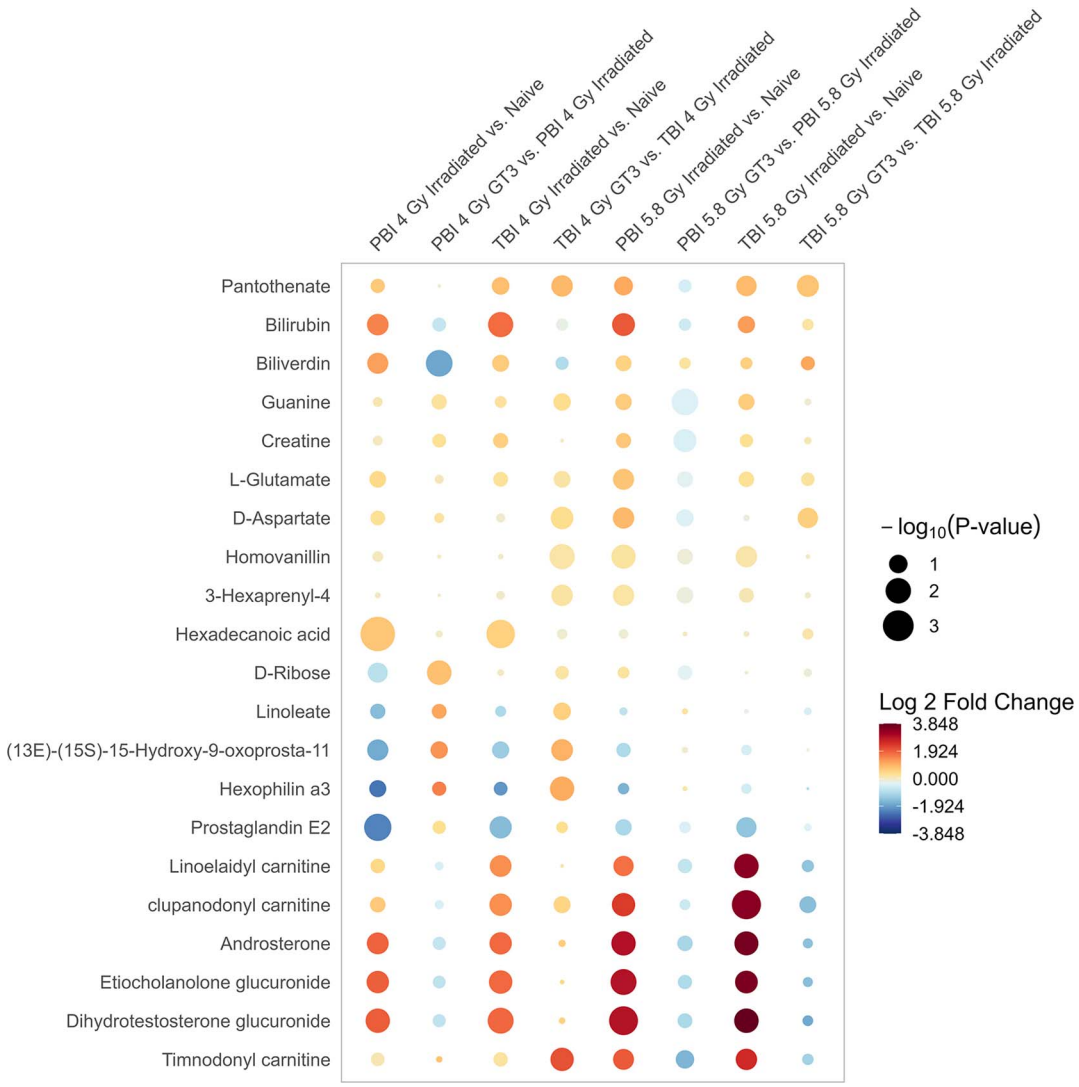

FIG. 4. Comparison of the effects of radiation and GT3 treatment on select metabolites in lung tissue.

ascorbate (Vitamin C) and aldarate metabolism, phosphatidylinositol phosphate metabolism, and porphyrin metabolism. As expected, irradiated animals exposed to 5.8 Gy TBI had the greatest amount of dysregulation, with a total of 33 significantly perturbed pathways. Only two pathways were significant in the 5.8 Gy TBI GT3-treated and irradiated group (parathion degradation and methionine and cysteine metabolism), both of which were uniquely affected. Select metabolites and pathways in spleen can be viewed in Supplementary Figs. 5 and 6 (https://doi.org/10.1667/RADE-23-00091.1.S2).

Overall, as was observed when studying the radiation effects, the greatest degree of dysregulation was generally observed in animals exposed to the higher dose of radiation (5.8 Gy) and TBI. Radioprotection from GT3 treatment was minimal in jejunum and kidney. The greatest degree of protection in these tissues was generally observed in animals exposed to either 4 Gy TBI or PBI. However, GT3 exerted robust protection in the lung and spleen, which was observed in both 4 Gy and 5.8 Gy groups.

DISCUSSION

To date, the U.S. FDA has not approved any MCMs for ARS to be administered prior to radiation exposure for prophylaxis; however, there are several such promising radiation MCMs under development. One of these agents is GT3, a vitamin E component that has shown antioxidant, anti-inflammatory, and neuroprotective properties, and which is currently being investigated as a radioprotector using murine and NHP models for FDA approval under the Animal Rule (*8*, *11*, *15*, *41*). We have presented metabolomic data generated in samples from NHPs exposed to two different doses of radiation and treated with GT3. Recently, we have reported metabolic changes in serum and tissue samples of ^{60}Co γ-TBI animals using murine (*42–44*) and NHP (*45–48*) models. We have also used a few radiation MCMs being developed for prophylactic use, such as amifostine (*42–44*), BIO 300 (*49*, *50*), Ex-Rad (*51*), and GT3 (*17*, *20*) to study metabolomics. Amifostine (*42–44*) studies are in a murine model while Ex-Rad (*51*) and GT3 (*17*) studies used an NHP model. In these studies, animals were exposed to lethal high doses of TBIs and results suggested restoration of radiation-induced alterations in metabolites in mice and NHPs. Other studies with BIO

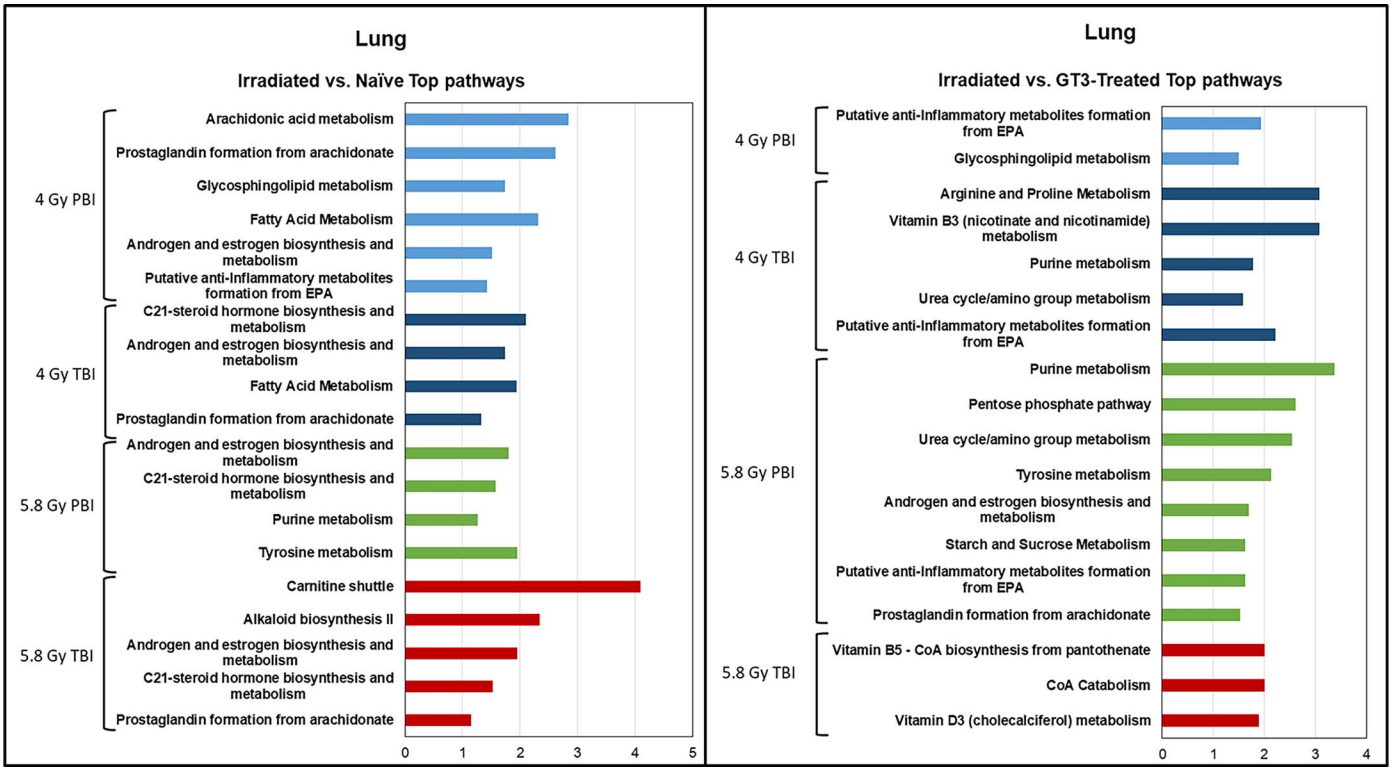

FIG. 5. Top significant pathways affected by radiation and GT3 treatment in lung tissue.

300 (*49*, *50*) and GT3 (*20*) using an NHP model demonstrated transient metabolic changes as a result of drug administration, and such changes reverted back to pre-drug exposure levels over time. A similar study was performed using NHPs exposed to 4 Gy TBI, which showed that the highest sensitivity for analyzing biomarkers was at 7 days postirradiation, and included carnitine and acetylcarnitine in urine and taurine, carnitine, and hypoxanthine in serum (*52*).

In an earlier study, we used serum samples from GT3-treated NHPs, either unirradiated or irradiated with 6.5 Gy TBI ($\sim LD_{50/60}$) (*17*, *20*), while in the current study, we have used various tissue samples from GT3-treated and irradiated NHPs exposed to 4.0 (sub-lethal dose) or 5.8 Gy ($\sim LD_{30/60}$) TBI or PBI. Additionally, a separate study was performed using several doses of ^{60}Co γ radiation and the NHP model, which demonstrated metabolite changes across six different doses of radiation (*53*). Using multi-omics platforms (metabolomics and proteomics), we used a logistic regression model to develop a 4-analyte panel to stratify unirradiated and irradiated NHPs with high accuracy across all radiation doses. That panel was comprised of acetylcarnitine, glycerophosphocholine (16:0/22:6), Serpin family A9, and suberylglycine, showing 2- to 4-fold elevation in serum samples of irradiated NHPs compared to pre-irradiation samples.

We expected to see a greater dysregulation of pathways and metabolites in a dose-dependent manner; additionally, we posited that total-body irradiation would induce greater metabolic dysregulation in the various tissues analyzed compared to PBI, due to 5% bone marrow sparing. For the most part, these assumptions were corroborated by the trends observed in metabolic perturbations. Both doses and exposure types of radiation-induced metabolic perturbations in the irradiated group when compared to naïve animals. Overall, metabolic perturbations increased proportionally with radiation dose. There was a large amount of variation in terms of the types and classes of metabolic perturbations and minimal specific patterns were noted between tissues. Similarly, dysregulation was higher in animals with TBI when compared to PBI, due to 5% bone marrow sparing in PBI. Minimal protection was observed in jejunum and kidney, while alleviation of radiation injury was more apparent in lung and spleen. Interestingly, C21-steroid hormone biosynthesis and metabolism was the only pathway that was significantly dysregulated by radiation exposure in all four tissues. This pathway is particularly notable, as it has been dysregulated by radiation exposure in other metabolomic studies and may play an important role in radiation injury (*51*). Prostaglandin formation from arachidonate and glycosphingolipid metabolism were also commonly and consistently dysregulated in various groups of the four tissues analyzed.

As for pathways that were significantly protected by GT3 treatment, jejunum and kidney had the fewest. In jejunum, pathways including glycosphingolipid metabolism, carnitine shuttle, bile acid biosynthesis, and pyrimidine

metabolism were commonly protected in GT3-treated and irradiated animals. In kidney, the drug metabolism – cytochrome P450 pathway was dysregulated in irradiated animals, but protected in GT3-treated 4 Gy TBI animals. Fewer metabolic pathways were disrupted in the kidney in comparison to the other tissues. This may be related to the mechanism of radiation-induced kidney injury which is thought to be due to cellular senescence, activation of the renin-angiotensin-aldosterone-system and vascular dysfunction that might contribute to renal injury that may not be responsive to the mode of radioprotection by GT3 (*40*). However, more robust protection was noted in both spleen and lung when compared to jejunum and kidney. In spleen, prostaglandin from the arachidonate pathway was protected at 4 Gy TBI. Interestingly, at 5.8 Gy PBI, several pathways were protected when compared to irradiated animals including the pentose phosphate pathway, ascorbate (vitamin C) and aldarate metabolism, chondroitin sulfate degradation, and pentose and glucoronate interconversions pathways. The majority of the pathways protected in spleen are related to glucose metabolism, suggesting GT3 may exert radioprotective effects by sparing these pathways from radiation-induced dysregulation.

Several pathways in the lung were protected by GT3 administration including purine metabolism, tyrosine metabolism, androgen and estrogen biosynthesis and metabolism, urea cycle/amino group metabolism, glutathione metabolism, aspartate and asparagine metabolism, putative anti-inflammatory metabolites formation from EPA, vitamin B5 metabolism, and CoA catabolism. Several of these pathways are involved in anti-inflammatory pathways that mitigate inflammation caused by radiation exposure. Additionally, when considering the long-term effects of ionizing radiation on lung, damage in the lung typically presents later (beyond the 30 days in this study) in the form of the delayed effects of acute radiation exposure (DEARE). DEARE in lung can result in pneumonitis and the development of fibrosis (*23*, *54*). The results of this study not only provide key insight into the early pathway perturbations that play a role in the development of DEARE in lung, but also in the potential of GT3 to mitigate damage to not only these metabolic pathways but also to the tissue in general. A transcriptomic study was recently performed in an NHP model using a supralethal dose of 12 Gy TBI and PBI (*15*). Similarly, robust alterations in lung transcriptomic profiles were observed as a result of irradiation, but GT3 treatment afforded limited protection in the lung at the supralethal dose. This further corroborates our observation that GT3 provides significant radioprotection at lower doses of radiation inducing H-ARS in lung, but it is unable to ameliorate radiation-induced damage at supralethal doses. Similar observations have been made with other studies using 12 Gy TBI/PBI and GT3 to examine changes in jejunal tissues in NHPs (*12*, *13*). However, it is important to note that GT3 is known to be minimally effective at protecting GI tissue after supralethal doses, and is not being developed for GI-ARS.

In summary, the results of this study suggest that GT3 provides robust protection to select metabolites and metabolic pathways from the deleterious effects of radiation to the lung and spleen, particularly at lower doses of radiation (e.g., 4.0 Gy) and after PBI, while providing minimal protection in the jejunum and kidney. To the best of our knowledge, this is the first report with GT3 in which metabolites were assessed in various tissues using PBI and TBI in an NHP model. Additional work is needed to determine the mechanistic action by which GT3 imparts its radioprotection, which will aid in its in further development as a MCM for use in radiation emergencies, whether from nuclear power plant accidents or from terrorist-related activities, and for national security preparedness and response.

SUPPLEMENTARY MATERIALS

Supplementary Table S1. A comprehensive list of all metabolites screened in this study.

Supplementary Table S2. Comparative metabolomics data of jejunum tissue between "irradiated vs. naïve" and "GT3 vs. irradiated" treatment groups for 4.0 and 5.8 Gy exposure to PBI (LINAC) and TBI (Cobalt-60).

Supplementary Table S3. Comparative metabolomics data of kidney tissue between "irradiated vs. naïve" and "GT3 vs. irradiated" treatment groups for 4.0 and 5.8 Gy exposure to PBI (LINAC) and TBI (Cobalt-60).

Supplementary Table S4. Comparative metabolomics data of lung tissue between "irradiated vs. naïve" and "GT3 vs. irradiated" treatment groups for 4.0 and 5.8 Gy exposure to PBI (LINAC) and TBI (Cobalt-60).

Supplementary Table S5. Comparative metabolomics data of spleen tissue between "irradiated vs. naïve" and "GT3 vs. irradiated" treatment groups for 4.0 and 5.8 Gy exposure to PBI (LINAC) and TBI (Cobalt-60).

Supplementary Table S6. Metabolomic pathway analysis results for the effects of radiation and GT3 treatment at SD30 in jejunum tissue. Analysis was performed with Mummichog software, version 2.06.

Supplementary Table S7. Metabolomic pathway analysis results for the effects of radiation and GT3 treatment at SD30 in kidney tissue. Analysis was performed with Mummichog software, version 2.06.

Supplementary Table S8. Metabolomic pathway analysis results for the effects of radiation and GT3 treatment at SD30 in lung tissue. Analysis was performed with Mummichog software, version 2.06.

Supplementary Table S9. Metabolomic pathway analysis results for the effects of radiation and GT3 treatment at SD30 in spleen tissue. Analysis was performed with Mummichog software, version 2.06.

Supplementary Fig. 1. Select metabolites illustrating the effects of radiation and GT3 treatment in jejunum tissue in each comparison.

Supplementary Fig. 2. Top significant pathways illustrating the effects of radiation and GT3 treatment in jejunum tissue in each comparison.

Supplementary Fig. 3. Select metabolites illustrating the effects of radiation and GT3 treatment in kidney tissue in each comparison.

Supplementary Fig. 4. Top significant pathways illustrating the effects of radiation and GT3 treatment in kidney tissue in each comparison.

Supplementary Fig. 5. Select metabolites illustrating the effects of radiation and GT3 treatment in spleen tissue in each comparison.

Supplementary Fig. 6. Top significant pathways illustrating the effects of radiation and GT3 treatment in spleen tissue in each comparison.

ACKNOWLEDGMENTS

The opinions or assertions contained herein are the private views of the authors and are not necessarily those of the Uniformed Services University of the Health Sciences or the Department of Defense. The authors report no conflicts of interest. The authors alone are responsible for the content and writing of this paper. The authors gratefully acknowledge the research support from the Congressionally Directed Medical Research Programs (W81XWH-15-C-0117, JW140032) and Defense Health Agency (75-13266) of the U.S. Department of Defense and the Uniformed Services University of the Health Sciences/Armed Forces Radiobiology Research Institute (grant # AFR-B4-10978) to VKS. The authors would like to acknowledge the Metabolomics Shared Resource at Georgetown University (Washington, DC), partially supported by NIH/NCI/CCSG grant P30-CA051008.

Received: May 18, 2023; accepted: September 27, 2023; published online: January 24, 2024

REFERENCES

1. Hall EJ, Giaccia AJ. Radiobiology for the Radiobiologist. 7th ed. Philadelphia, PA: Lippincott Williams and Wilkins; 2012.
2. Singh VK, Seed TM. A review of radiation countermeasures focusing on injury-specific medicinals and regulatory approval status: part I. Radiation sub-syndromes, animal models and FDA-approved countermeasures. Int J Radiat Biol 2017 Sep; 93(9):851-69.
3. Singh VK, Newman VL, Romaine PL, Hauer-Jensen M, Pollard HB. Use of biomarkers for assessing radiation injury and efficacy of countermeasures. Expert Rev Molecular Diagn 2016 Dec 8; 16: 65-81.
4. Armed Forces Radiobiology Research Institute. Medical Management of Radiological Casualities. Fourth ed. Bethesda, MD, U.S.A: Armed Forces Radiobiology Research Institute; 2013.
5. Singh VK, Seed TM. Radiation countermeasures for hematopoietic acute radiation syndrome: growth factors, cytokines and beyond. Int J Radiat Biol 2021 Aug 31; 97(11):1526-47.
6. U.S. Food and Drug Administration. Animal Rule approvals. U.S. Food and Drug Administration; 2022.
7. Singh VK, Beattie LA, Seed TM. Vitamin E: Tocopherols and tocotrienols as potential radiation countermeasures. J Radiat Res 2013 May 8; 54(6):973-88.
8. Singh VK, Hauer-Jensen M. Gamma-tocotrienol as a promising countermeasure for acute radiation syndrome: Current status. Int J Mol Sci 2016; 17(5):e663.
9. Berbee M, Fu Q, Boerma M, Sree Kumar K, Loose DS, Hauer-Jensen M. Mechanisms underlying the radioprotective properties of gamma-tocotrienol: comparative gene expression profiling in tocol-treated endothelial cells. Genes Nutr 2012 Jan; 7(1):75-81.
10. Berbee M, Fu Q, Boerma M, Wang J, Kumar KS, Hauer-Jensen M. gamma-Tocotrienol ameliorates intestinal radiation injury and reduces vascular oxidative stress after total-body irradiation by an HMG-CoA reductase-dependent mechanism. Radiat Res 2009 May; 171(5):596-605.
11. Singh VK, Kulkarni S, Fatanmi OO, Wise SY, Newman VL, Romaine PL, et al. Radioprotective efficacy of gamma-tocotrienol in nonhuman primates. Radiat Res 2016 Mar; 185(3):285-98.
12. Garg S, Garg TK, Miousse IR, Wise SY, Fatanmi OO, Savenka AV, et al. Effects of gamma-tocotrienol on partial-body irradiation-induced intestinal injury in a nonhuman primate model. Antioxidants 2022 Sep 25; 11(10):1895.
13. Garg S, Garg TK, Wise SY, Fatanmi OO, Miousse IR, Savenka AV, et al. Effects of gamma-tocotrienol on intestinal injury in a GI-specific acute radiation syndrome model in nonhuman primate. Int J Mol Sci 2022 Apr 22; 23(9):4643.
14. Garg TK, Garg S, Miousse IR, S.Y. W, Carpenter AD, Fatanmi OO, et al. Gamma-tocotrienol modulates total-body irradiation-induced hematopoietic injury in a nonhuman primate model. Int J Mol Sci 2022; 23:16170.
15. Singh VK, Seed TM. Development of gamma-tocotrienol as a radiation medical countermeasure for the acute radiation syndrome: Current status and future perspectives. Expert Opin Investig Drugs 2023 Jan 19; 32:25-35.
16. Fendler W, Malachowska B, Meghani K, Konstantinopoulos PA, Guha C, Singh VK, Chowdhury D. Evolutionarily conserved serum microRNAs predict radiation-induced fatality in nonhuman primates. Sci Transl Med 2017 Mar 01; 9(379):eaal2408.
17. Pannkuk EL, Laiakis EC, Fornace AJ, Jr., Fatanmi OO, Singh VK. A metabolomic serum signature from nonhuman primates treated with a radiation countermeasure, gamma-tocotrienol, and exposed to ionizing radiation. Health Phys 2018 Jul; 115(1):3-11.
18. Rosen E, Fatanmi OO, Wise SY, Rao VA, Singh VK. Tocol prophylaxis for total-body irradiation: A proteomic analysis in murine model. Health Phys 2020 Jul; 119(1):12-20.
19. Rosen E, Fatanmi OO, Wise SY, Rao VA, Singh VK. Gamma-tocotrienol, a radiation countermeasure, reverses proteomic changes in serum following total-body gamma irradiation in mice. Sci Rep 2022 Mar 1; 12(1):3387.
20. Cheema AK, Mehta KY, Fatanmi OO, Wise SY, Hinzman CP, Wolff J, Singh VK. A Metabolomic and lipidomic serum signature from nonhuman primates administered with a promising radiation countermeasure, gamma-tocotrienol. Int J Mol Sci 2018 Dec 28; 19(1):79.
21. Cheema AK, Byrum SD, Sharma NK, Altadill T, Kumar VP, Biswas S, et al. Proteomic changes in mouse spleen after radiation-induced injury and its modulation by gamma-tocotrienol. Radiat Res 2018 Aug 2; 190:449-63.
22. U.S. Food and Drug Administration. Animal Rule information. 2022.
23. Singh VK, Olabisi AO. Nonhuman primates as models for the discovery and development of radiation countermeasures. Expert Opin Drug Discov 2017 May 05; 12(7):695-709.
24. Singh VK, Carpenter AD, Janocha BL, Petrus SA, Fatanmi OO, Wise SY, Seed TM. Radiosensitivity of rhesus nonhuman primates: Consideration of sex, supportive care, body weight and age at time of exposure. Expert Opin Drug Discov 2023 Apr 18; 18(7): 797-814.
25. Chaudhry MA. Biomarkers for human radiation exposure. J Biomed Sci 2008 Sep; 15(5):557-63.
26. Sullivan JM, Prasanna PG, Grace MB, Wathen LK, Wallace RL, Koerner JF, Coleman CN. Assessment of biodosimetry methods for

a mass-casualty radiological incident: medical response and management considerations. Health Phys 2013 Dec; 105(6):540-54.

27. Singh VK, Seed TM, Cheema AK. Metabolomics-based predictive biomarkers of radiation injury and countermeasure efficacy: Current status and future perspectives. Expert Rev Molecular Diagn 2021 May 22; 21:641-54.

28. Pannkuk EL, Fornace AJ, Jr., Laiakis EC. Metabolomic applications in radiation biodosimetry: exploring radiation effects through small molecules. Int J Radiat Biol 2017 Jan 12; 93(10): 1151-76.

29. Shakyawar SK, Mishra NK, Vellichirammal NN, Cary L, Helikar T, Powers R, et al. A review of radiation-induced alterations of multi-omic profiles, radiation injury biomarkers, and countermeasures. Radiat Res 2023 Nov 11; 199(1).

30. Singh VK, Fatanmi OO, Wise SY, Carpenter AD, Olsen CH. Determination of lethality curve for cobalt-60 gamma-radiation source in rhesus macaques using subject-based supportive care. Radiat Res 2022 Dec 1; 198(6):599-614.

31. National Research Council of the National Academy of Sciences. Guide for the care and use of laboratory animals. 8th ed. Washington, DC: National Academies Press; 2011.

32. Vellichirammal NN, Sethi S, Pandey S, Singh J, Wise SY, Carpenter AD, et al. Lung transcriptome of nonhuman primates exposed to total- and partial-body irradiation. Mol Ther Nucleic Acids 2022 Sep 13; 29:584-98.

33. Li Y, Singh J, Varghese R, Zhang Y, Fatanmi OO, Cheema AK, Singh VK. Transcriptome of rhesus macaque (*Macaca mulatta*) exposed to total-body irradiation. Sci Rep 2021 Mar 18; 11(1):6295.

34. American Veterinary Medical Association. AVMA Guidelines for the Euthanasia of Animals: 2020 Edition. 2020.

35. R Core Team. R: A language and environment for statistical computing. 2017.

36. Smith CA, O'Maille G, Want EJ, Qin C, Trauger SA, Brandon TR, et al. METLIN: a metabolite mass spectral database. Ther Drug Monit 2005 Dec; 27(6):747-51.

37. Gil-de-la-Fuente A, Godzien J, Saugar S, Garcia-Carmona R, Badran H, Wishart DS, et al. CEU mass mediator 3.0: A metabolite annotation tool. J Proteome Res 2019 Feb 1; 18(2):797-802.

38. Wishart DS, Feunang YD, Marcu A, Guo AC, Liang K, Vazquez-Fresno R, et al. HMDB 4.0: the human metabolome database for 2018. Nucleic Acids Res 2018 Jan 4; 46(D1):D608-D17.

39. Li S, Park Y, Duraisingham S, Strobel FH, Khan N, Soltow QA, et al. Predicting network activity from high throughput metabolomics. PLoS Comput Biol 2013; 9(7):e1003123.

40. Klaus R, Niyazi M, Lange-Sperandio B. Radiation-induced kidney toxicity: molecular and cellular pathogenesis. Radiat Oncology. 2021 Feb 25; 16(1):43.

41. Ghosh SP, Kulkarni S, Hieber K, Toles R, Romanyukha L, Kao TC, et al. Gamma-tocotrienol, a tocol antioxidant as a potent radioprotector. Int J Radiat Biol 2009 Jul; 85(7):598-606.

42. Crook A, De Lima Leite A, Payne T, Bhinderwala F, Woods J, Singh VK, Powers R. Radiation exposure induces cross-species temporal metabolic changes that are mitigated in mice by amifostine. Sci Rep 2021 Jul 7; 11(1):14004.

43. Cheema AK, Li Y, Girgis M, Jayatilake M, Fatanmi OO, Wise SY, et al. Alterations in tissue metabolite profiles with amifostine-prophylaxed mice exposed to gamma radiation. Metabolites 2020 May 21; 10(5):211.

44. Cheema AK, Li Y, Girgis M, Jayatilake M, Simas M, Wise SY, et al. Metabolomic studies in tissues of mice treated with amifostine and exposed to gamma-radiation. Sci Rep 2019 Oct 30; 9(1):15701.

45. Cheema AK, Hinzman CP, Mehta KY, Hanlon BK, Garcia M, Fatanmi OO, Singh VK. Plasma derived exosomal biomarkers of exposure to ionizing radiation in nonhuman primates. Int J Mol Sci 2018 Nov 1; 19(11):3427.

46. Pannkuk EL, Laiakis EC, Garcia M, Fornace AJ, Jr., Singh VK. Nonhuman primates with acute radiation syndrome: Results from a global serum metabolomics study after 7.2 Gy total-body irradiation. Radiat Res 2018 Sep 5; 190(5):576-83.

47. Pannkuk EL, Laiakis EC, Singh VK, Fornace AJ. Lipidomic signatures of nonhuman primates with radiation-induced hematopoietic syndrome. Sci Rep 2017 Aug 29; 7(1):9777.

48. Cheema AK, Mehta KY, Rajagopal MU, Wise SY, Fatanmi OO, Singh VK. Metabolomic studies of tissue injury in nonhuman primates exposed to gamma-radiation. Int J Mol Sci 2019 Jul 9; 20(13):3360.

49. Li Y, Girgis M, Jayatilake M, Serebrenik AA, Cheema AK, Kaytor MD, Singh VK. Pharmacokinetic and metabolomic studies with a BIO 300 oral powder formulation in nonhuman primates. Sci Rep 2022 Aug 5; 12(1):13475.

50. Cheema AK, Mehta KY, Santiago PT, Fatanmi OO, Kaytor MD, Singh VK. Pharmacokinetic and metabolomic studies with BIO 300, a nanosuspension of genistein, in a nonhuman primate model. Int J Mol Sci 2019 Mar 12; 20(5):1231.

51. Li Y, Girgis M, Wise SY, Fatanmi OO, Seed TM, Maniar M, et al. Analysis of the metabolomic profile in serum of irradiated nonhuman primates treated with Ex-Rad, a radiation countermeasure. Sci Rep 2021 Jun 1; 11(1):11449.

52. Pannkuk EL, Laiakis EC, Gill K, Jain SK, Mehta KY, Nishita D, et al. Liquid chromatography-mass spectrometry-based metabolomics of nonhuman primates after 4 Gy total body radiation exposure: Global effects and targeted panels. J Proteome Res 2019 May 3; 18(5):2260-9.

53. Cheema AK, Li Y, Moulton J, Girgis M, Wise SY, Carpenter A, et al. Identification of novel biomarkers for acute radiation injury using multiomics approach and nonhuman primate model. Int Journal Radiat Oncol Biol Phys 2022 Oct 1; 114(2):310-20.

54. Bansal S, Bansal S, Fish BL, Li Y, Xu X, Fernandez JA, et al. Analysis of the urinary metabolic profiles in irradiated rats treated with Activated Protein C (APC), a potential mitigator of radiation toxicity. Int J Radiat Biol 2023:1-10.